PHILOSOPHICAL TRANSACTIONS OF THE ROYAL SOCIETY A
MATHEMATICAL, PHYSICAL & ENGINEERING SCIENCES

InSb Devices: Transphasors with High Gain, Bistable Switches and Sequential Logic Gates

A. C. Walker, F. A. P. Tooley, M. E. Prise, J. G. H. Mathew, A. K. Kar, M. R. Taghizadeh and S. D. Smith

Phil. Trans. R. Soc. Lond. A 1984 **313**, 249-256
doi: 10.1098/rsta.1984.0103

Phil. Trans. R. Soc. Lond. A **313**, 249–256 (1984)
Printed in Great Britain

InSb devices: transphasors with high gain, bistable switches and sequential logic gates

By A. C. Walker, F. A. P. Tooley, M. E. Prise, J. G. H. Mathew, A. K. Kar, M. R. Taghizadeh and S. D. Smith, F.R.S.

Department of Physics, Heriot-Watt University, Riccarton, Currie, Edinburgh EH14 4AS, U.K.

InSb etalons operated at 77 K and illuminated by CO lasers (5.5 μm) exhibit continuous wave (c.w.) optical bistability. A wide range of experiments have been performed to further the basic characterization of these devices and to demonstrate their various potential applications. The latter include signal amplification, modulation and, with external switching, the construction of logic gates. Two devices on a single etalon have now been coupled to form a simple all-optical circuit.

New results have also been obtained with InSb at room temperature with pulsed CO_2 lasers (10.6 μm).

1. Introduction

The purpose of this paper is to review the recent experimental results in the optical bistability (o.b.) project at Heriot–Watt University obtained with InSb as the nonlinear medium. Liquid-nitrogen cooled InSb and CO lasers have proved to be an extremely useful combination in both the study of optical bistability and the demonstration of practical bistable devices. In addition, InSb with CO_2 laser illumination has permitted the demonstration of bistable switching at room temperature.

2. Basic measurements

From an experimental point of view we are motivated in making measurements of the nonlinearities of the basic material by the desire to predict in advance the input–output characteristic of any bistable-type device we choose to fabricate. It has been clear for some time that the simplest plane-wave theory is inadequate, as illustrated in the comparison with experiment shown in figure 1*a*, *b*. Before resorting to the complexity of a full 2D theory (taking into account the laser focal-spot irradiance profile, diffraction, refraction and carrier diffusion (see, for example, Firth *et al.*, this symposium)) it is worth considering how far simple improvements to the uniform-illumination plane-wave theory can take us towards realistic modelling of experimental characteristics.

Firstly, the dependence of Δn, the radiation-induced change in refractive index, upon irradiance, I, should be generalized beyond more than the simple $n_2 I$ linear dependence. Density-dependent recombination rates and saturation of the contribution of each excess carrier-pair to Δn are both mechanisms by which this dependence will become more complex. $\Delta n(I)$ could either be calculated from a full microscopic theory (see, for example, Wherrett, this symposium) or, alternatively, deduced from an experimental o.b. characteristic, provided that *all* other experimental parameters are known (including the temperature and absorption effects discussed below).

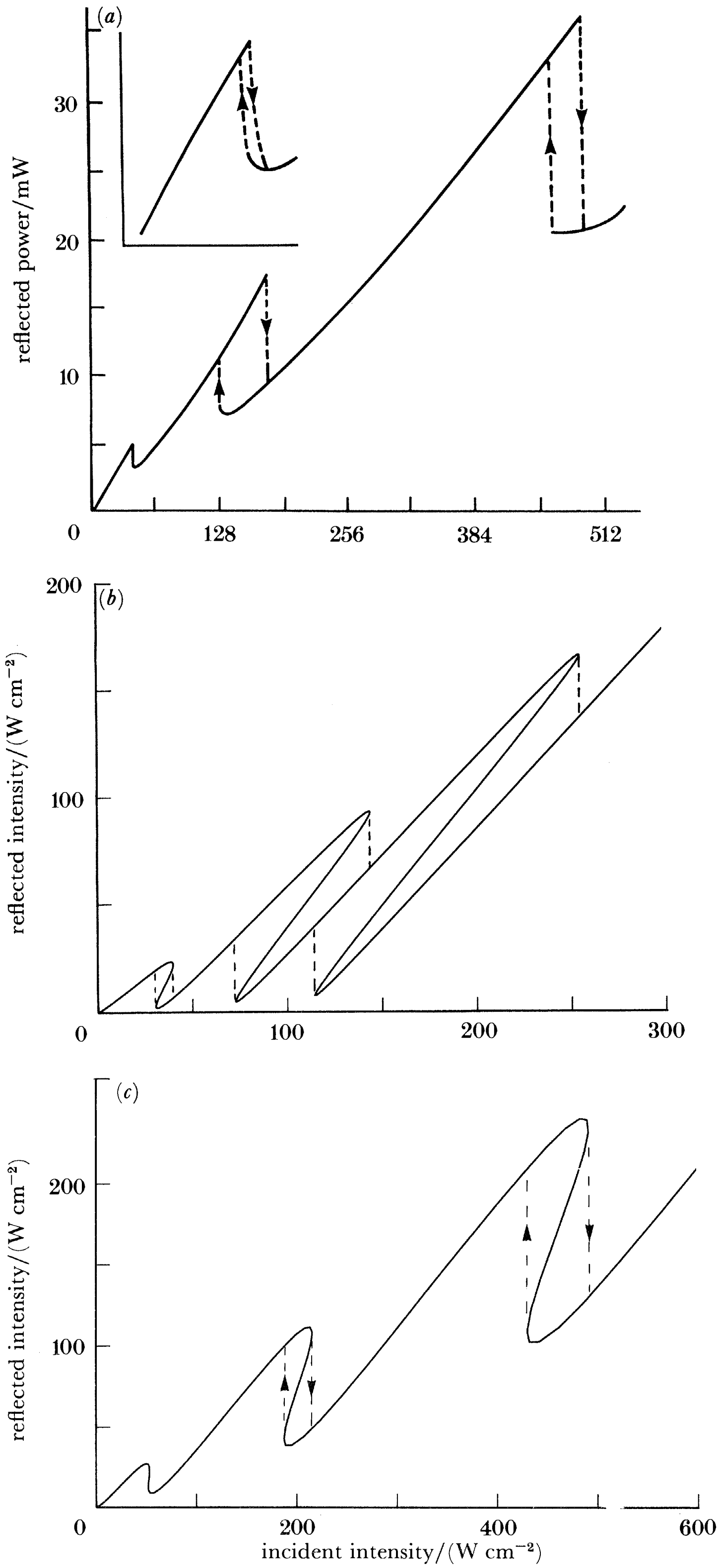

FIGURE 1. Input–output characteristics (reflection) for an InSb etalon: (*a*) experimental result (temperature 77 K, cavity length 210 μm, natural reflectivity 36 %, laser line 1818.8 cm^{-1}); (*b*) calculated from simple plane-wave theory; (*c*) calculated from the improved plane-wave theory described in the text, with $\sigma = 1.9 \times 10^{-18}$ cm^3. The inset in (*a*) shows first-order bistability magnified.

PHILOSOPHICAL TRANSACTIONS OF THE ROYAL SOCIETY A MATHEMATICAL, PHYSICAL & ENGINEERING SCIENCES

Secondly, the irradiance dependence of the absorption coefficient, α, should be included. This may be a saturation phenomenon, associated with the microscopic origins of the refractive nonlinearity itself, or an induced absorption effect, for example due to rapidly increasing free-carrier absorption.

Finally, thermal effects should be taken into account. In addition to the linear refractive index's being temperature dependent, the position of the band edge also moves with temperature. Thus for a band-gap resonantly enhanced nonlinearity both $\Delta n(I)$ and α can change significantly for a temperature change of only a few kelvins.

We are currently working towards including these three factors in a modified plane-wave model of InSb optically bistable devices. The following considers each in turn.

A compromise assumption for determining $\Delta n(I)$ is that saturation of the contribution of each excess carrier-pair can be neglected and hence

$$\Delta n(I) = \sigma \Delta N(I). \tag{1}$$

That is, Δn is directly proportional to the excess carrier-pairs, ΔN, with a constant of proportionality σ (Miller *et al.* 1981); $\Delta N(I)$ then remains to be determined. This requires a knowledge of carrier recombination rates. A review of published experimental data for excess-carrier lifetimes in n-InSb at 77–100 K shows considerable spread of values. However, there is a clear trend showing shortening lifetimes, T_1, at higher carrier densities (over 5×10^{15} $\mathrm{cm^{-3}}$) and an empirical relation can be deduced of the form

$$T_1^{-1} = r_1 + r_2(N_0 + \Delta N), \tag{2}$$

where N_0 is the dark carrier density and ΔN the excess carrier density. This relation implies a monomolecular, e.g. trap, recombination at low carrier densities, evolving to a bimolecular, e.g. radiative, recombination process at higher densities. A fit to the data can be obtained by using $r_1 = 1.5\times 10^{6}\ \mathrm{s^{-1}}$ and $r_2 = 1.5\times 10^{-10}\ \mathrm{cm^3\ s^{-1}}$, both rates being accurate to about $\pm 50\,\%$.

Using (2) for T_1, the equilibrium excess carrier density can be calculated for any internal irradiance, I (in watts per square centimetre), from $\Delta N = \alpha_0\, T_1\, I/h\nu$. Thus $\Delta N(I)$, and hence the refractive index change, can be obtained from

$$\Delta N(I) = \frac{[(r_1 + r_2 N_0)^2 + 4 r_2 \alpha_0 I/h\nu]^{\frac{1}{2}} - (r_1 + r_2 N_0)}{2 r_2}, \tag{3}$$

where α_0 is the carrier generating absorption coefficient (in reciprocal centimetres) and $h\nu$ the photon energy (in joules).

It is assumed in the above that α_0 is not significantly saturated at these irradiance levels. This is consistent with experimental measurements of absorption as a function of irradiance performed on other samples from the batch currently being used to fabricate bistable devices. These results, shown in figure 2, demonstrate an increase in transmission losses with increasing irradiance, and appear to be consistent with a simple model based on additional absorption being induced by the generated free-carrier pairs. Assuming equal electron and hole concentrations, free-carrier absorption is dominated by the direct intra-valence-band hole transition. The hole absorption cross section is $\sigma_p = 2.5\times 10^{-15}\ \mathrm{cm^2}$ at 77 K in InSb (Kurnick & Powell 1959). The total absorption coefficient is then given by

$$\alpha = \alpha_0 + \Delta N(I)\, \sigma_p. \tag{4}$$

PHILOSOPHICAL TRANSACTIONS OF THE ROYAL SOCIETY A MATHEMATICAL, PHYSICAL & ENGINEERING SCIENCES

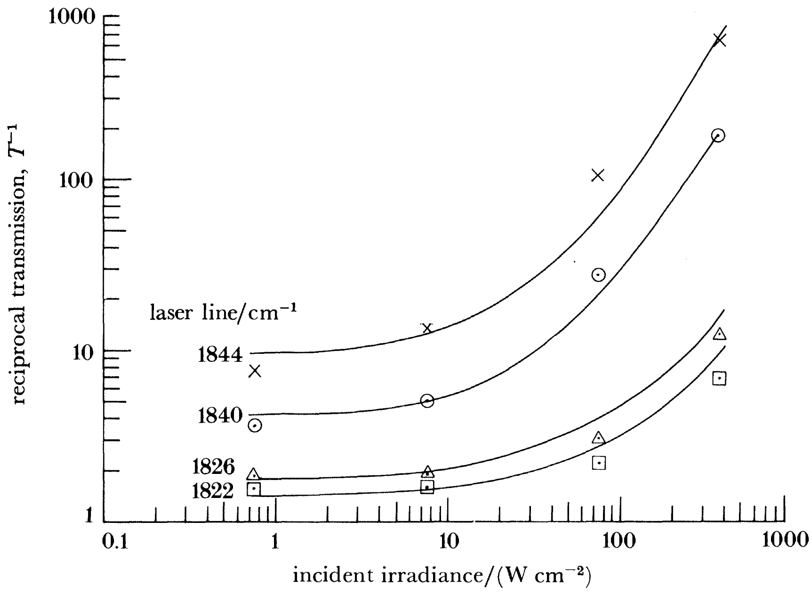

FIGURE 2. Transmission of a 0.5 mm InSb sample at 77 K as a function of incident irradiance. Points are experimental results, curves are calculated (free carrier absorption and temperature).

To simplify the integration across the sample thickness, the relation $\Delta N(I) = \alpha_0 T_{\text{eff}} I_0/h\nu$ was used, where T_{eff} is an effective carrier lifetime for the average ΔN values deduced from the full equation (3). Thus the transmission, T, through a sample of thickness L can be obtained:

$$T = \frac{\exp(-\alpha_0 L)}{1+\{1-\exp(-\alpha_0 L)\} I_0 T_{\text{eff}} \sigma_{\text{p}}/h\nu}, \tag{5}$$

where I_0 is the incident irradiance.

By using this relation, plus a small correction allowing for (measured) heating effects, the curves in figure 2, showing an approximate fit with the experimental results, were calculated. It is important to note that this calculation assumes that every photon absorbed, as a result of the band tail, creates an electron–hole pair. This is despite the photon energy deficit relative to the band gap. The mechanism for this band-tail absorption process in the region commonly used in these bistability experiments (typically $\alpha_0 \approx 5$ to $40\ \text{cm}^{-1}$) is not understood. Furthermore, in contrast to this, absorption *saturation* is the dominant absorption nonlinearity near 77 K for photon energies *above* the band gap (Nurmikko 1976) whereas below 5 K this is true both below and above the band gap (Miller *et al.* 1978; Lavallard *et al.* 1976). Although induced absorption of the type observed here has been reported (Miller *et al.* 1978) it has not been previously measured this close to the band edge.

The remaining factor to be considered is the effect of sample heating caused by the incident laser beam. This is discussed more fully by Tooley *et al.* (this symposium) in a paper on incoherent–coherent switching. Detailed modelling of thermal effects is complicated by the need for full knowledge of the heat diffusion and conduction properties of the sample–mount assembly and is not considered further here.

It has been found, by using (3) to calculate the excess carrier density, and hence both Δn from (1) and the total absorption from (2), that the input–output characteristic calculated from plane-wave theory gives a much closer fit to the experimental result. This is shown in figure

1 *c*, where σ has been taken to be 1.9×10^{-18} cm^3 (equivalent to $n_2 = 0.3$ cm^2 kW^{-1} at low ΔN). Further improvements in modelling such characteristics will probably require a fuller 2D calculation.

3. Transphasor action

By adjusting the initial detuning from resonance of the InSb etalon the transmission characteristic can be made to have a steeply sloped single-valued region, giving high differential gain. This permits the construction of a transphasor amplifier. By using a separate 3 μW, 5.5 μm wavelength chopped beam as a probe, pulse amplification of up to 1.3×10^4 has been observed from a single device (Tooley *et al.* 1983). It should be noted that there is no requirement for the signal to be coherent with the bias beam in this application, as was demonstrated by using orthogonally polarized beams with equal success.

4. Response speeds

The signal frequency in the high-gain transphasor experiment was limited to *ca.* 1 kHz by mechanical chopping rates. It is important that the upper bandwidth limit of the InSb transphasor be determined. Direct observations of the switching times obtained by very slowly sweeping the input power give an upper limit of *ca.* 2 μs for both switch-on and switch-off. (Much faster switch-on times should be possible with more intense, fast-rising pulses, as implied by successful switching with 35 ps Nd:YAG laser pulses (Seaton *et al.* 1983).) To investigate the higher frequency response of a transphasor-type device, a 1.3 μm laser diode, capable of being modulated at over 10 MHz, has been used as the signal source. The experimental arrangement is shown in figure 3, together with the reflection characteristic employed. No

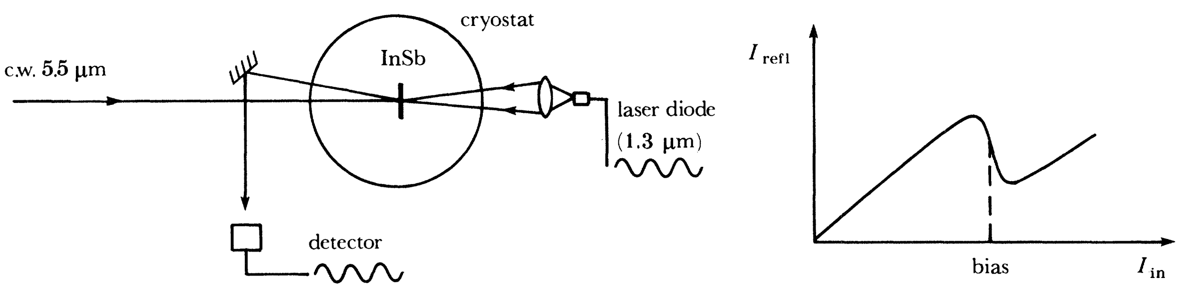

Figure 3. Experimental layout and operating condition for the demonstration of high-frequency cross-wavelength modulation (1.3 and 5.5 μm). A gain of *ca.* 1 is observed between 0.2 and 1.0 MHz.

attempt was made to achieve gain in this instance. With the device biased to the centre of the negative slope region, the signal on the 1.3 μm beam incident on the rear face of the sample induced linearly proportional modulation on the reflected 5.5 μm beam. From initial experiments only it appears that no significant roll-off in response occurs in the frequency band so far studied, up to *ca.* 1 MHz.

5. Cross-wavelength modulation and switching

In addition to the 1.3 μm laser diode a wide range of other sources have now been used to switch or modulate the 5 μm InSb o.b.-switch or transphasor. These include visible wavelengths, which are of particular interest to potential image-processing applications. For example, with the laser diode in figure 3 replaced by a 10 mW He–Ne laser, both switching and modulation of the 5.5 μm reflected beam by coherent visible radiation have been demonstrated. Alternatively, by using a photographic flash unit, incoherent–coherent switching with white light has been studied (Tooley *et al.* this symposium). Table 1 summarizes these and other experiments.

Table 1. Cross-wavelength modulation and switching of an InSb o.b. device pumped at 5.5 μm

wavelength, etc. (source)	operation mode	gain	frequency
5.5 μm, 3 μW (CO laser)	switching	1.3×10^4	*ca.* kilohertz
1.3 μm, 3 mW (laser diode)	switching	*ca.* 1	single pulse
	modulation	*ca.* 1	*ca.* megahertz
1.06 and 0.53 μm, 5 nJ (Nd:YAG laser)	switching	—	single pulse (35 ps)
0.633 μm, 10 mW (He–Ne laser)	switching, modulation	*ca.* 1	3 kHz
white light (camera flash)	switching	—	single pulse

6. Demonstrations of sequentially coupled logic elements

An experiment in which the transmission change through one bistable InSb device was used to switch a second has been reported (Smith & Tooley 1984). Recently we have coupled two devices together working in their reflection mode and, more significantly, with both gates operating adjacent to each other on a single InSb etalon. The experimental geometry is shown in figure 4, together with the results obtained. The two gates were addressed from opposite sides of the sample and were separated by about 0.5 mm, i.e. about 2.5 focal-spot diameters. The reflection from gate 1 was directed at gate 2. By biasing gate 2 to just below its switch point the following sequence was demonstrated, as reproduced in figure 4. Firstly, as the input power to gate 1 is increased the reflected power becomes sufficient to switch on gate 2 (low reflection state). A further increase, however, causes gate 1 to switch on. The consequent drop in reflected power simultaneously causes gate 2 to turn off. Finally, a further increase in input power can eventually turn gate 2 back on once more. The range of input powers over which gate 2 remains on is determined by its initial bias condition. This device represents an XNOR gate and is also close to a flip–flop configuration, the latter simply requiring the reflection from gate 2 to be directed back at gate 1. Finally, by using transmission feedback, or by adding a third switch, an oscillator could be constructed.

Altogether, the feasibility of a wide range of logic devices has been demonstrated. For example, with a single active element only, both AND and OR gates can be made by using the transmission mode, while NAND and NOR gates are obtained by operating in the reflection mode. The device described above demonstrated a two-element XNOR gate, while the first element alone acted as an XOR gate. Finally, of course, a bistable characteristic provides a memory element. We have now reached the point where we can start to build simple all-optical circuits.

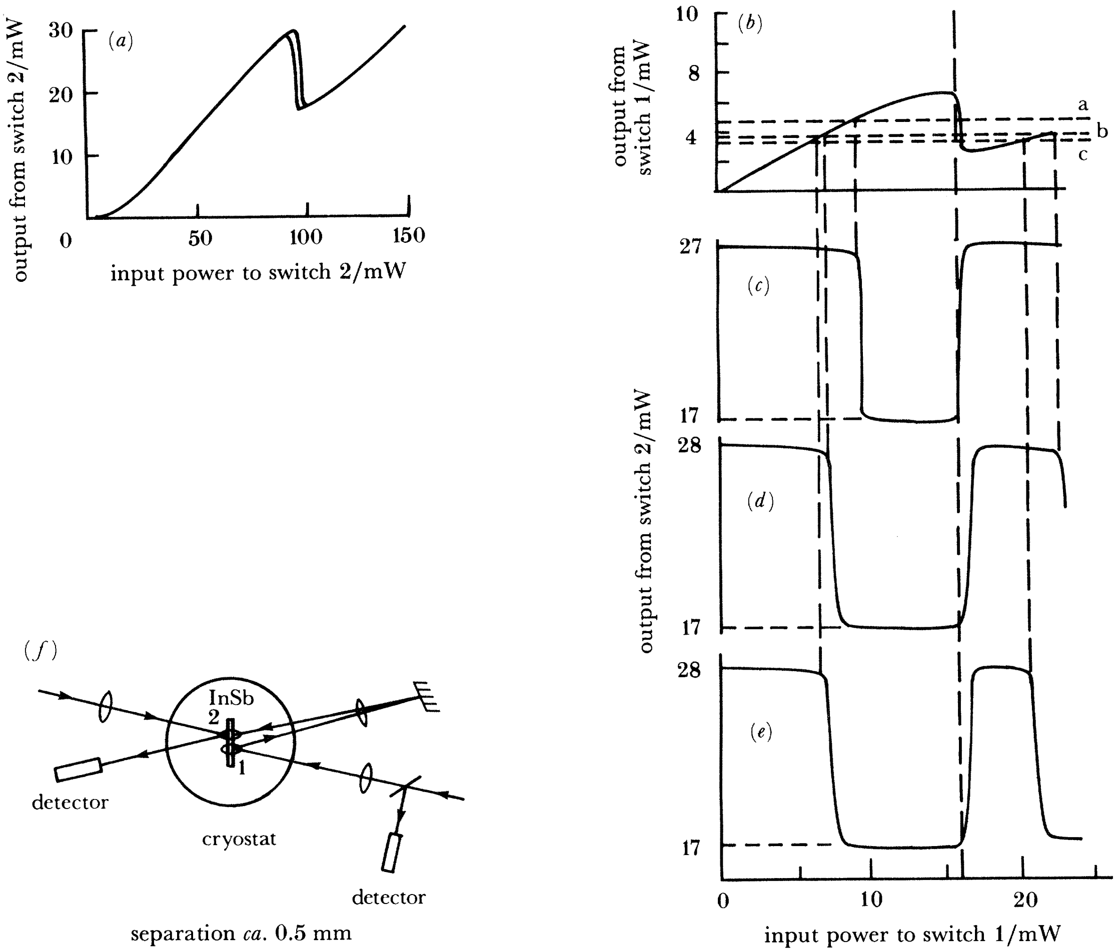

FIGURE 4. Two coupled o.b. switches on a single InSb element. (*f*) Experimental layout. (*a*, *b*) Input–output characteristics of the two switches; (*c*–*e*) input–output characteristics of the combination, showing the result of increasing approach of the initial bias of switch 2 to its switch point.

7. ROOM-TEMPERATURE InSb RESULTS

The results of initial optical bistability studies on room-temperature InSb have already been published (Kar *et al.* 1983). In these experiments free carriers are excited across the 0.18 eV band gap with 10.6 μm (CO_2 laser) radiation by a two-photon process. Recent results have been obtained with longer, *ca.* 3 μs, duration pulses to minimize the dynamic effects of the rise and fall of incident power. In addition, small-area pinholes mounted directly onto the samples have been used to define an area of uniform illumination at a specific point on the device. This should permit more direct comparison of experimental results with plane-wave theory. Controlled variation of the initial detuning is achieved by angular adjustment of the sample. The pinhole ensures that all measurements are made on the same part of the sample, avoiding any uncertainties caused by material or surface-finish non-uniformity. Figure 5 includes an example of the transmission characteristic, which shows clear hysteresis. Care must be taken in claiming true bistability before completion of a full analysis of *all* the dynamic effects. Figure 5 also plots the switching irradiance as a function of initial detuning and shows, at least qualitatively, the expected trend.

PHILOSOPHICAL TRANSACTIONS OF THE ROYAL SOCIETY A MATHEMATICAL, PHYSICAL & ENGINEERING SCIENCES

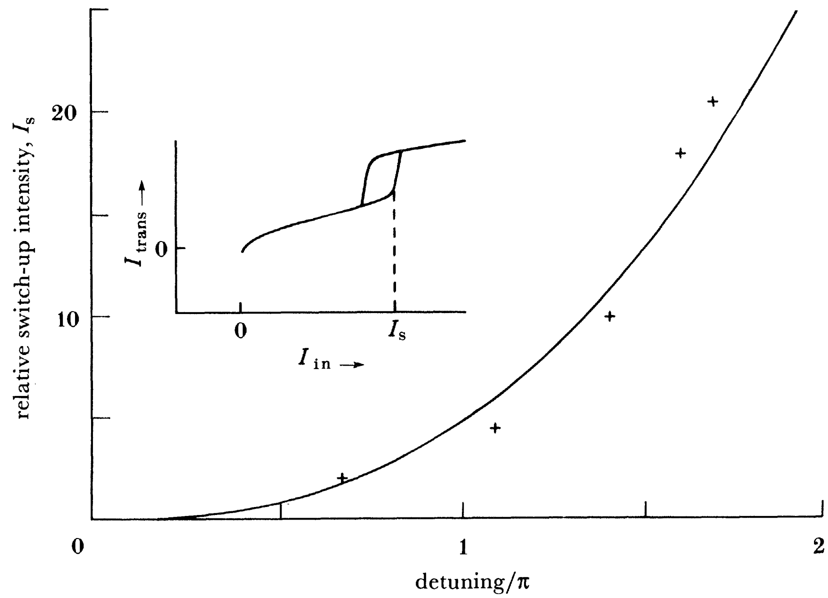

FIGURE 5. Switch-up irradiance as a function of initial detuning for a room-temperature InSb device operating at 10.6 μm wavelength. Inset shows a typical input–output characteristic (transmission).

8. Conclusions

This experimental programme can be summarized under three main headings: the physics of the nonlinearity and associated parameters, e.g. the form of $\Delta n(I, T)$ and $\alpha(I, T)$; the development and characterization of single devices, e.g. switches, transphasors and modulators, and the coupling of devices to develop photonic logic. Future work is directed at taking these InSb devices further, including the investigation of possible waveguide geometries.

It now seems possible to iterate a significant number of all-optical circuit elements and to demonstrate a simple processor.

The authors acknowledge the assistance of Dr H. A. Mackenzie and Mr J. Reid in these experiments, the contribution of Mr N. Ross to sample preparation and the general support of Dr B. S. Wherrett. The 1.3 μm laser diodes were generously provided by S.T.C. Ltd., Harlow.

References

Kar, A. K., Mathew, J. G. H., Smith, S. D., Davis, B. & Prettl, W. 1983 *Appl. Phys. Lett.* **42**, 334.
Kurnick, S. W. & Powell, J. M. 1959 *Phys. Rev.* **116**, 597.
Lavallard, P., Bichard, R. & Benoit á la Guillaume, C. 1976 *Phys. Rev.* B **16**, 2804.
Miller, D. A. B., Mozolowski, M. H., Miller, A. & Smith, S. D. 1978 *Optics Commun.* **27**, 133.
Miller, D. A. B., Seaton, C. T., Prise, M. E. & Smith, S. D. 1981 *Phys. Rev. Lett.* **47**, 197.
Nurmikko, A. V. 1976 *Optics Commun.* **16**, 365.
Seaton, C. T., Smith, S. D., Tooley, F. A. P., Prise, M. E. & Taghizadeh, M. R. 1983 *Appl. Phys. Lett.* **42**, 131.
Smith, S. D. & Tooley, F. A. P. 1984 In *Proc. Topical Meeting on Optical Bistability, Rochester, U.S.A.* (In the press.)
Tooley, F. A. P., Smith, S. D. & Seaton, C. T. 1983 *Appl. Phys. Lett.* **43**, 807.